Development of *N*-[4-[6-(Isopropylamino)pyrimidin-4-yl]-1,3-thiazol-2-yl]-*N*-methyl-4-[11C]methylbenzamide for Positron Emission Tomography Imaging of Metabotropic Glutamate 1 Receptor in Monkey Brain

Masayuki Fujinaga,[†] Tomoteru Yamasaki,[†,‡] Jun Maeda,[†] Joji Yui,[†] Lin Xie,[†] Yuji Nagai,[†] Nobuki Nengaki,[†,§] Akiko Hatori,[†] Katsushi Kumata,[†] Kazunori Kawamura,[†] and Ming-Rong Zhang*,[†]

[†]Molecular Imaging Center, National Institute of Radiological Sciences, 4-9-1 Anagawa, Inage-ku, Chiba 263-8555, Japan
[‡]Graduate School of Pharmaceutical Sciences, Tohoku University, Aoba-ku, Sendai 980-8574, Japan
[§]SHI Accelerator Service Co. Ltd., 5-9-11 Kitashinagawa, Shinagawa-ku, Tokyo 141-8686, Japan

Ⓢ Supporting Information

ABSTRACT: Three novel 4-substituted benzamides have been synthesized as potential ligands for the positron emission tomography (PET) imaging of metabotropic glutamate 1 (mGlu1) receptor in the brain. Of these compounds, *N*-(4-(6-(isopropylamino)pyrimidin-4-yl)-1,3-thiazol-2-yl)-*N*,4-dimethylbenzamide (**4**) exhibited the highest binding affinity (K_i = 13.6 nM) for mGlu1 and was subsequently labeled with carbon-11. In vitro autoradiography using rat brain sections showed that [11C]**4** binding was consistent with the distribution of mGlu1, with high specific binding in the cerebellum and thalamus. PET studies with [11C]**4** in monkey showed a high brain uptake and a kinetic profile suitable for quantitative analysis. Pretreatment with a mGlu1-selective ligand **16** largely decreased the brain uptake, indicating high in vivo specific binding of [11C]**4** to mGlu1. In metabolite analysis, only unchanged [11C]**4** was found in the brain. [11C]**4** is a useful PET ligand for the imaging and quantitative analysis of mGlu1 in monkey brain and merits further evaluation in humans.

11: R = SnBu₃
[11C]4: R = 11CH₃
[11C]CH₃I, Pd₂(dba)₃

i.v. injection of [11C]4 into monkey
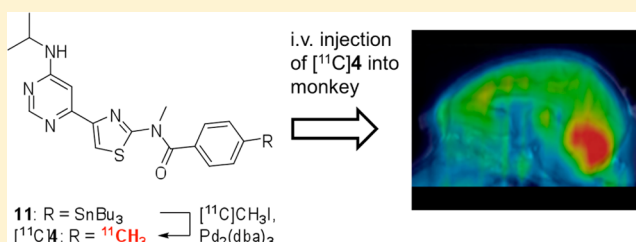
INTRODUCTION

Glutamate is one of the most abundant excitatory neurotransmitters in the central nervous system (CNS) and acts on a variety of different receptors, all of which have the potential to be involved in many abnormal and pathological conditions of the CNS. Glutamate receptors are characterized as ionotropic (*N*-methyl-D-aspartate, *α*-amino-3-hydroxy-5-methyl-4-isoxazolepropionic acid, and kainite receptors) or metabotropic types. On the basis of their sequence homology, coupling mechanisms to G-proteins, and pharmacological activities, metabotropic glutamate (mGlu) receptors have been divided into three groups including eight subtypes.[1,2] Group I of the mGlu receptors contains mGlu1 and mGlu5 which are involved in the regulation of ion channels, synaptic transmission, and synaptic plasticity, the last of which has been related to memory and learning.[3−5] There have been several reports suggesting that mGlu1 is a drug development target for the treatment of pain, cerebellar ataxia, Parkinson's disease, stroke, epilepsy, anxiety, and mood disorders caused by neurodegeneration in the CNS.[2−11]

Positron emission tomography (PET) with a radioligand is an advanced molecular imaging modality for studying the living human brain. The technique is useful for studying brain receptors, enzymes, and plaques associated with pathophysiology and therapeutic interventions.[12] PET imaging can be used to elucidate the function and mechanism of mGlu1 involved in health and disorders, and this information could be used for the development of new drugs targeting mGlu1.

Several mGlu1 ligands have been labeled with carbon-11 (11C, half-life = 20.4 min) or fluorine-18 (18F, half-life = 109.8 min), and their potential for the PET imaging of mGlu1 was evaluated.[13−17] However, despite their high binding affinity for mGlu1 in vitro, PET studies with these radioligands showed low specific signals even in the mGlu1-rich brain regions. Furthermore, the radiolabeled metabolites of some of these ligands entered the brain, raising nonspecific binding signals in the brain. As a result of these problems, to date, no PET ligands have been used for the clinical study of mGlu1 in the human brain.

Recently, we developed two specific and selective radioligands for mGlu1, including 4-[18F]fluoro-*N*-[4-(6-(isopropylamino)-pyrimidin-4-yl)-1,3-thiazol-2-yl]-*N*-methylbenzamide ([18F]FITM, [18F]**1**) and *N*-[4-(6-(isopropylamino)pyrimidin-4-yl)-1,3-thiazol-2-yl]-4-[11C]methoxy-*N*-methylbenzamide ([11C]ITMM, [11C]**2**) (Figure 1).[18−20] PET studies with each radioligand in rodents and primates revealed acceptable brain
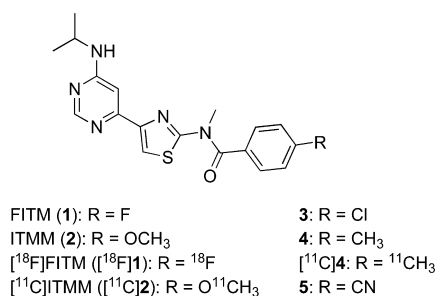
Figure 1. Chemical structures of **1**–**5** and their labeled compounds.

uptakes and sizable mGlu1-specific signals in the brain regions. In vivo specific binding of [18F]**1** and [11C]**2** was observed not only in mGlu1-rich regions of the brain such as the cerebellum but also in mGlu1-moderate and low regions of the brain, including the thalamus, cingulate cortex, and striatum.[18,19] Consequently, both of these PET ligands have been scheduled for clinical trials in two separate facilities to evaluate their behavior in the human brain.

There are disadvantages associated with the use of [18F]**1**, including slow kinetics in the brain.[19] A PET study in rats showed a continuously increased uptake of radioactivity in the cerebellum until 90 min after the injection of [18F]**1**, while the uptake in the monkey brain increased until 30 min and then declined at a very slow rate. In addition, the radiosynthesis of [18F]**1** was low yielding (14 ± 3%, decay-corrected), because the reaction of the nitro precursor with [18F]F⁻ at 180 °C resulted in significant decomposition of the nitro precursor.[20] The efficient separation of [18F]**1** from the nitro precursor and byproducts using high performance liquid chromatography (HPLC) also represented a challenging task. On the other hand, PET studies using [11C]**2** showed clearance of uptake in the brain, demonstrating the improved kinetics of [11C]**2** over [18F]**1**. However, metabolite analysis with [11C]**2** revealed that around 20% of the total radioactivity observed in the rat brain 60 min after the injection represented the radiolabeled metabolite, which would complicate quantitative analysis for mGlu1.[18] Desmethylation of the [11C]methoxy group in [11C]**2** was identified as one of the possible in vivo metabolizing routes that resulted in brain-penetrating radiolabeled metabolites, such as [11C]methanol or its analogues.

The aim of this study was to develop an improved PET ligand for the quantitative analysis of mGlu1 by overcoming the shortcomings of [18F]**1** and [11C]**2**. By use of compound **1** as a lead compound, the fluoro group of its benzamide moiety was

replaced with chloro, methyl, and cyano groups to give the new benzamide analogues **3**–**5**, respectively (Figure 1). We envisaged that the binding affinities of these new compounds **3**–**5** for mGlu1 would be similar to that of compound **1** because of the bioisosteric properties of the substituent groups and fluorine. Furthermore, these substituent groups attached to the benzene ring may be stable for in vivo metabolism. Compounds **3**–**5** could be labeled with [11C]methyl iodide ([11C]MeI) or hydrogen [11C]cyanide.

Herein, we describe the development of *N*-[4-[6-(isopropylamino)pyrimidin-4-yl]-1,3-thiazol-2-yl]-*N*-methyl-4-[11C]methylbenzamide ([11C]**4**) (Figure 1) as a promising PET ligand for the in vivo imaging and quantitative analysis of mGlu1 in brain.

■ RESULTS AND DISCUSSION

Synthesis of Unlabeled Compounds. Compounds **3**–**5** were synthesized from the *N*-methylthiazole **6**, as shown in Scheme 1. Compound **6** was prepared according to a procedure described previously.[18] The subsequent reaction of **6** with the appropriate 4-substituted benzoyl chlorides afforded **7**–**9** in chemical yields of 68–90%. The reactions of **7**–**9** with isopropylamine provided **3**–**5** in 59–67%, respectively (Supporting Information Figure 1).

In Vitro Binding Assays. The affinity of compounds **3**–**5** for mGlu1 was measured using the binding assay with the mGlu1-selective radioligand [18F]**1** in rat brain homogenate. As shown in Table 1, these compounds exhibited high affinity for mGlu1, with K_i values in the range of 13–27 nM. Compound **4** displayed the highest affinity (K_i = 13.6 nM), with a value 2-fold higher than those of **3** and **5**. These results suggested that the presence of relatively small substituents, such as the methyl and fluoro groups, at the 4-position of the benzene ring provided a better fit for the binding site of the mGlu1 domain. Although the affinity of **4** was slightly weaker than that of **1** (K_i = 5.4 nM), its value was similar to that of **2** (K_i = 12.6 nM).[18] We recently reported the mGlu1 density in different regions of the rat brain to be 36.3 nM in the thalamus, 27.5 nM in the hippocampus, and 22.2 nM in the striatum.[21] The affinity of **4** for mGlu1 was therefore considered to be adequate for the visualization of brain mGlu1 using PET.
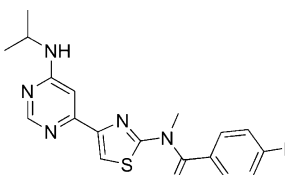
The binding affinities of **3**–**5** for mGlu5, the other subtype of group I mGlu receptors, were also measured using a competing assay with the mGlu5-selective radioligand 3-(6-methylpyridin-2-ylethynyl)cyclohex-2-enone-*O*-[11C]methyloxime[22] ([11C]-ABP688, [11C]**10**; Supporting Information Figure 2). As shown in Table 1, the affinities of **3**–**5** for mGlu5 were found to be >10000 nM, demonstrating that the replacement of the

Scheme 1. Syntheses of 3–5[a]
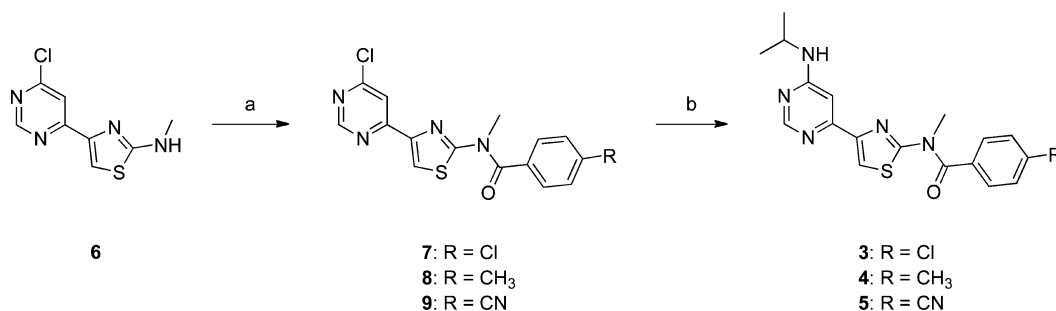
[a]Reagents and conditions: (a) 4-substituted benzoyl chlorides, Et₃N, toluene, 100 °C, 3–8 h; (b) isopropylamine, K₂CO₃, 1,4-dioxane, 80 °C, 7–8 h.

Table 1. In Vitro Affinity and Lipophilicity

		ligand affinity			lipophilicity	
		mGluRl		mGluR5		
compd	R	IC$_{50}$ (nM)	K_i (nM)	IC$_{50}$ (nM)	cLogD [a]	log D
3	Cl	47.0 ± 8.5	22.2 ± 8.6	>10000	2.62	c
4	CH$_3$	26.5 ± 5.9	13.6 ± 3.4	>10000	2.67	1.74
5	CN	64.7 ± 19.4	27.3 ± 2.8	>10000	2.39	c
1	F	13.9 ± 1.2[b]	5.4 ± 1.2[b]	>10000[b]	2.35[b]	1.45[b]
2	OCH$_3$	32.7 ± 1.2[b]	12.6 ± 1.2[b]	>10000[b]	2.64[b]	2.57[b]

[a]cLogD values were calculated with Pallas 3.4 software. [b]Value was from ref 18. [c]Not measured.

Scheme 2. Synthesis of Precursor 11 and Radiosynthesis of [^{11}C]4[a]
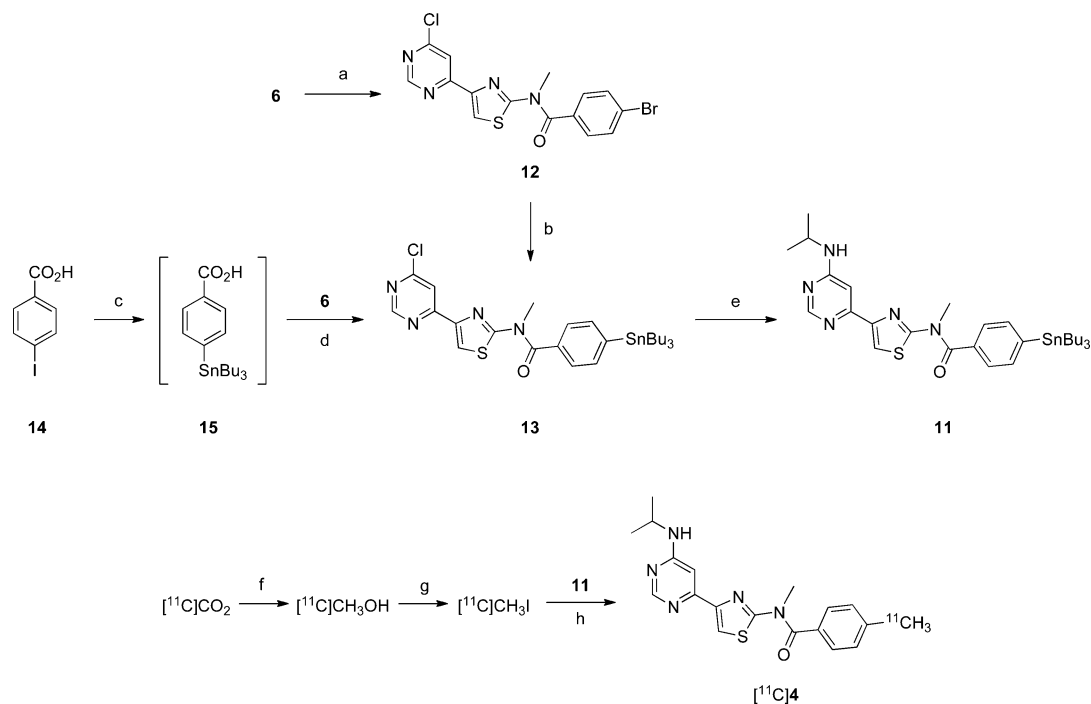
[a]Reagents and conditions: (a) 4-bromobenzoyl chloride, Et$_3$N, toluene, 100 °C, 6 h; (b) (n-Bu$_3$Sn)$_2$, Pd(PPh$_3$)$_4$, K$_2$CO$_3$, toluene, 100 °C, 24 h; (c) (n-Bu$_3$Sn)$_2$, Pd(PPh$_3$)$_4$, LiCl, 1,4-dioxane, reflux, 17 h; (d) BOP, Et$_3$N, 1,4-dioxane, 50 °C, 20 h; (e) isopropylamine, K$_2$CO$_3$, 1,4-dioxane, 80 °C, 6 h; (f) LiAlH$_4$, THF, −15 °C, 2 min; (g) hydroiodic acid, 180 °C, 2 min; (h) Pd$_2$(dba)$_3$, P(o-tol)$_3$, CuCl, K$_2$CO$_3$, DMF, 80 °C, 5 min.

fluoro group in **1** with the alternative groups did not have any adverse impact on the high selectivity for mGlu1. A high selectivity for mGlu1 over mGlu5 is a desirable characteristic for a prospective PET ligand for mGlu1.

Computation and Measurement of Lipophilicity. A moderate lipophilicity is an important physiochemical property required for development of a promising brain imaging agent capable of achieving the high brain uptake via passage through the blood−brain barrier (BBB), without incurring nonspecific binding and for avoiding troublesome lipophilic brain-penetrating metabolites.[23] The computed values of lipophilicities at pH 7.4 (cLogD) for **3**−**5** were 2.39−2.67 (Table 1). Although these values were slightly higher than the value calculated for [^{18}F]**1**

(cLogD = 2.35), they were within the range of 2−3, which is the range generally considered to be suitable for brain imaging.[23] Following the labeling of **4** with ^{11}C, its lipophilicity (log D) was measured using the Shake Flask method.[24] The experimentally determined log D value of [^{11}C]**4** was 1.74. The precise reason for the difference between the cLogD and log D values of [^{11}C]**4** remains unclear.

■ RADIOLABELING

Compound **4** was selected as the target for labeling with ^{11}C to evaluate the potential of [^{11}C]**4** as a PET ligand for the imaging and quantification of mGlu1 because of its high binding affinity and selectivity for mGlu1 and suitable lipophilicity.
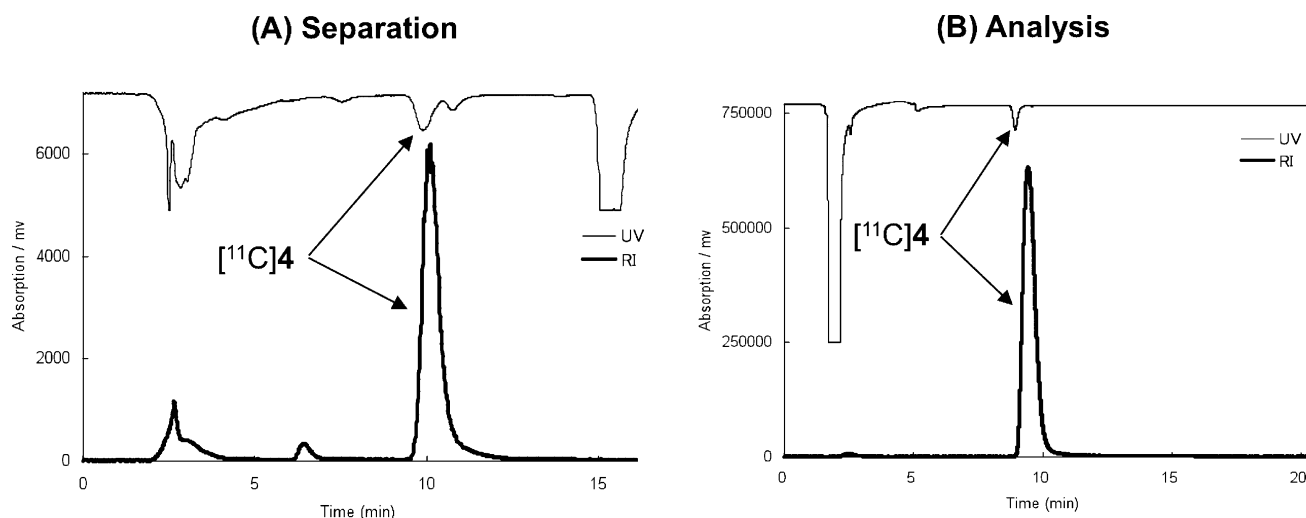
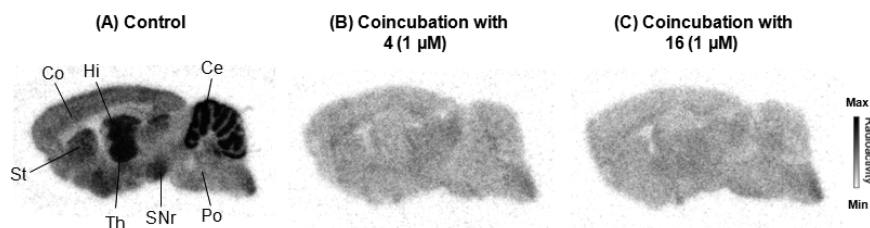**Figure 2.** Chromatograms from the HPLC separation (A) and analysis (B) used in the radiosynthesis of $[^{11}C]$**4**.

Figure 3. Representative in vitro autoradiographic images of rat brain sections with $[^{11}C]$**4** (7.4 MBq, 40 pmol): (A) $[^{11}C]$**4** only; (B) $[^{11}C]$**4** with unlabeled **4** (1 μM); (C) $[^{11}C]$**4** with **16** (1 μM). Abbreviations are as follows: Ce, cerebellum; Th, thalamus; Hi, hippocampus (CA3); St, striatum; SNr, substantia nigra pars reticulate; Po, pons; Co, cerebral cortex.

Arylstannanes are known to be susceptible to the direct introduction of a $[^{11}C]$methyl group to their benzene ring via cross-coupling reaction with a palladium(0) complex and $[^{11}C]$MeI.[25] Arylstannane **11** was prepared as a precursor for our radiolabeling strategy involving the C-^{11}C coupling reaction of **11** with $[^{11}C]$MeI (Scheme 2). However, stannylation of the bromo analogue **12** with bis(tributyltin) in the presence of tetrakis(triphenylphosphine)palladium(0) $[Pd(PPh_3)_4]$ gave **13** in a low yield of 4%. Increases in the reaction time and the addition of LiCl did not improve the yield of **13**.

Another route was used for the synthesis of **11** starting from 4-iodobenzoic acid (**14**). Compound **14** was reacted with bis(tributyltin) in the presence of $Pd(PPh_3)_4$ to give **15**.[26,27] The reaction between **15** and **6** in the presence of (benzotriazol-1-yloxy)tris(dimethylamino)phosphonium hexafluorophosphate (BOP) gave **13** in 20% yield from **14**. Treatment of **13** with isopropylamine afforded **11** in 71% yield (Supporting Information Figure 1). This route guaranteed an adequate supply of **11** as a precursor for the radiosynthesis.

The radiosynthesis of $[^{11}C]$**4** was performed using a homemade automated synthesis system.[28] Crucially, the precursor solution, containing a mixture of **11**, tris-(dibenzylideneacetone)dipalladium $[Pd_2(dba)_3]$, P(o-tol)$_3$, copper(I) chloride, K_2CO_3, and N,N-dimethylformamide (DMF), in which a Pd complex was formed, was prepared immediately prior to the start of the radiosynthesis process. When the mixture was exposed to air, the Pd complex would immediately decompose and any subsequent attempt at the C-$[^{11}C]$methylation of **11** would fail. Thus, air was carefully removed from the system by purging N_2 gas through the precursor solution before introducing it to synthesis module.

$[^{11}C]$MeI for radiosynthesis was prepared and trapped in the precursor solution (Scheme 2). The reaction mixture was heated at 80 °C for 5 min. Separation of this mixture by reversed phase HPLC gave $[^{11}C]$**4** in a radiochemical yield of $19 \pm 9\%$ ($n = 11$) (decay-corrected) based on $[^{11}C]CO_2$ (Figure 2A).

Starting from 19.6−28.9 GBq $[^{11}C]CO_2$, 1.2−1.6 GBq $[^{11}C]$**4** was produced within 31 min ($n = 11$) of averaged synthesis time from the end of bombardment (EOB). In the final product solution, the specific activity and radiochemical purity of $[^{11}C]$**4** were 70−170 GBq/μmol and higher than 99% at the end of synthesis (EOS) (Figure 2B). The radioactive product did not show radiolysis at room temperature until 120 min after formulation, indicating radiochemical stability within the duration of at least one PET scan. The analytical results of $[^{11}C]$**4** were in compliance with our in-house quality control/assurance specifications for radiopharmaceuticals.

In Vitro Autoradiography. Figure 3 shows the in vitro autoradiographic images of the rat brain sections obtained from the co-incubation of $[^{11}C]$**4** with the vehicle (A), 1 μM unlabeled **4** (B), or 1 μM mGlu1-selective antagonist 3,4-dihydro-2H-pyrano[2,3-b]quinolin-7-yl)-(cis-4-methoxycyclohexyl)-methanone[29] (JNJ16259685, **16**; Supporting Information Figure 2) (C). In the control section (A), the distribution pattern of radioactivity was heterogeneous, with a high concentration of radioactivity in the cerebellum and thalamus. Moderate concentrations were detected in the hippocampus, striatum, substantia nigra pars reticulate, and cerebral cortex. The lowest radioactive signal was seen in the pons. This pattern was consistent with the regional distribution pattern of mGlu1 observed in the rat brain.[13,20,30,31] By co-incubation with unlabeled **4** or **16**, the radioactive signals in the brain sections

Table 2. Biodistribution (%ID/g Tissue, Mean $\pm$ SE, n = 4) of [^{11}C]4 in Mice

tissue	1 min	5 min	15 min	30 min	60 min	90 min
blood	3.09 ± 0.21	1.27 ± 0.06	0.37 ± 0.03	0.14 ± 0.01	0.05 ± 0.00	0.02 ± 0.01
heart	4.93 ± 0.30	1.28 ± 0.03	0.27 ± 0.02	0.09 ± 0.01	0.06 ± 0.01	0.01 ± 0.01
lung	5.48 ± 0.68	2.56 ± 0.15	0.86 ± 0.14	0.31 ± 0.03	0.20 ± 0.02	0.12 ± 0.09
liver	11.47 ± 0.84	11.38 ± 0.58	4.89 ± 0.74	1.43 ± 0.13	0.51 ± 0.02	0.30 ± 0.06
spleen	1.74 ± 0.18	0.93 ± 0.04	0.29 ± 0.08	0.07 ± 0.01	0.02 ± 0.01	0.02 ± 0.00
pancreas	4.48 ± 0.38	1.23 ± 0.05	0.30 ± 0.07	0.06 ± 0.00	0.03 ± 0.01	0.04 ± 0.02
kidney	11.12 ± 0.70	4.41 ± 0.19	1.32 ± 0.16	0.56 ± 0.10	0.22 ± 0.04	0.11 ± 0.01
small intestine	10.07 ± 0.90	66.76 ± 13.43	41.52 ± 6.00	16.53 ± 3.77	17.46 ± 3.61	7.09 ± 0.68
large intestine	1.28 ± 0.25	1.03 ± 0.10	1.20 ± 0.21	2.32 ± 0.81	1.98 ± 0.38	7.02 ± 1.80
muscle	2.59 ± 0.69	0.96 ± 0.13	0.23 ± 0.02	0.13 ± 0.05	0.07 ± 0.02	0.17 ± 0.08
testis	1.07 ± 0.15	0.63 ± 0.01	0.41 ± 0.04	0.22 ± 0.02	0.13 ± 0.03	0.14 ± 0.01
brain	2.19 ± 0.10	2.58 ± 0.04	1.99 ± 0.10	1.59 ± 0.09	1.04 ± 0.13	0.62 ± 0.08

decreased significantly (B and C). The in vitro results, demonstrating that [^{11}C]4 had high specific binding to mGlu1 in the rat brain, merit further in vivo evaluation using PET to assess the potential of [^{11}C]4 for mGlu1 imaging in living brains.

Biodistribution Study. The distribution of radioactivity in the whole body of a mouse was measured at six experimental time points (1, 5, 15, 30, 60, and 90 min) after the injection of [^{11}C]4 (Table 2). At 1 min, a high uptake of radioactivity (>3% injected dose per gram of wet tissue, %ID/g) was shown to immediately reach a peak in the blood, heart, lung, liver, pancreas, kidney, and small intestine. After the initial uptake, radioactivities in the most tissues decreased rapidly, while the level in the liver and small intestine remained high until 5 min and then decreased rapidly. The radioactivity in the large intestine continued to increase until 90 min. This distribution pattern suggested that the hepatobiliary and intestinal reuptake pathways may dominate the whole-body distribution with the rapid washout of radioactivity from the body following the injection of [^{11}C]4.

In the brain, the target tissue of the current study, the uptake of radioactivity was higher than in most of the other tissues sampled, reaching a peak of 2.58%ID/g at 5 min after the injection and thereafter retaining a relatively high level. This result provided a prerequisite of a useful PET ligand for brain imaging. The considerable brain uptake for [^{11}C]4 was attributed in part to its lipophilicity (cLogD = 2.67).

PET Studies in Monkey. Figure 4 shows the summed PET/ magnetic resonance images of monkey brain acquired between 10 and 90 min after injection of [^{11}C]4 in a baseline and two pretreatment experiments in the same monkey. The baseline images (A, B) revealed a ranking order of radioactive signals with cerebellum > thalamus ≈ cingulate cortex > pons, as identified by the co-registration of the brain structure with an MRI scan. The distribution of radioactivity corresponded to the distribution pattern of mGlu1 in the monkey brain.[15,16] Pretreatment with unlabeled 4 (1 mg/kg, C, D) or the mGlu1-selective antagonist 16 (3 mg/kg, E, F) almost abolished the radioactive signals, with the distribution of radioactivity becoming fairly uniform throughout the brain.

Figure 5 shows the time−activity curves (TACs) of [^{11}C]4 in monkey brain for the baseline (A) and pretreatment experiments with 4 (B) or 16 (C). The radioactivity entered brain well after the injection of [^{11}C]4 (A). The maximum standardized uptake values (SUVs) in the mGlu1-rich regions were 1.2 for the cerebellum, 0.8 for the thalamus, and 0.9 for the cingulate cortex and occurred around 20 min. In the other brain regions examined, including the hippocampus, putamen, caudate, and pons, the peaks were observed around 10 min. Following these
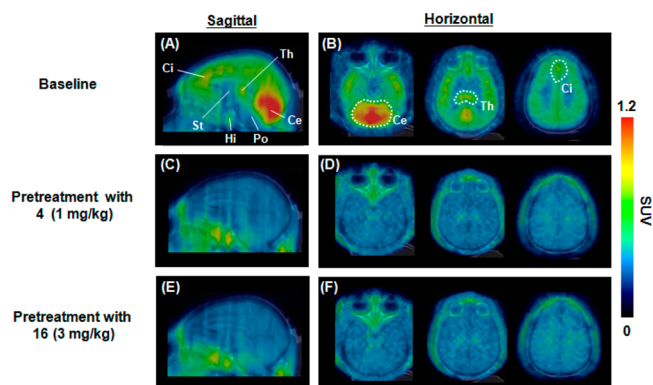

Figure 4. Representative PET/MRI images of the isoflurane-anesthetized monkey brains. PET images (A−F) were generated by summing from the scans taken from10 to 90 min: (A, C, E) sagittal images; (B, D, F) horizontal images; (A, B) [^{11}C]4 (185 MBq, 5 nmol) only; (C, D) [^{11}C]4 (200 MBq, 5 nmol) after treatment with 4 (1 mg/kg); (E, F) [^{11}C]4 (220 MBq, 6 nmol) after treatment with 16 (3 mg/kg). Abbreviations are as follows: Ce, cerebellum; Th, thalamus; Hi, hippocampus; St, striatum; Ci, cingulate cortex; Po, pons.

peaks, the radioactivity declined in all regions. Pretreatment of the monkey with 4 reduced the levels of radioactivity observed in the whole brain (Figure 5B). Although a high initial uptake was seen in the whole brain after the injection of [^{11}C]4, which might be partially dependent on blood radioactivity, radioactivity in the brain regions, including the cerebellum, thalamus, and cingulate cortex, was reduced to a similar and low level. This result suggested that 1 mg/kg 4 was enough to occupy the binding site of [^{11}C]4 in the brain. Pretreatment with 16 provided a result (Figure 5C) similar to that observed in the pretreatment with 4. Significant inhibition was observed without difference in radioactivity concentrations among the brain regions. The difference in the PET images and the TACs between the baseline and pretreatment with 4 or 16 implied the presence of a high proportion of specific binding to mGlu1 in the monkey brain, especially in the cerebellum, thalamus, and cingulate cortex.

In the current study, the distribution volume ratio (DVR)[32] data for [^{11}C]4 across several different regions of the monkey brain were noninvasively acquired using the TACs in the blocking experiment with unlabeled 4 (Table 3). The area under the curve (AUC) of radioactivity in the baseline ($\int C_T$) was used to estimate specific and nondisplaceable uptake, with the latter including nonspecific binding in the brain tissue plus free [^{11}C]4. DVR in each brain region was estimated under the equilibrium
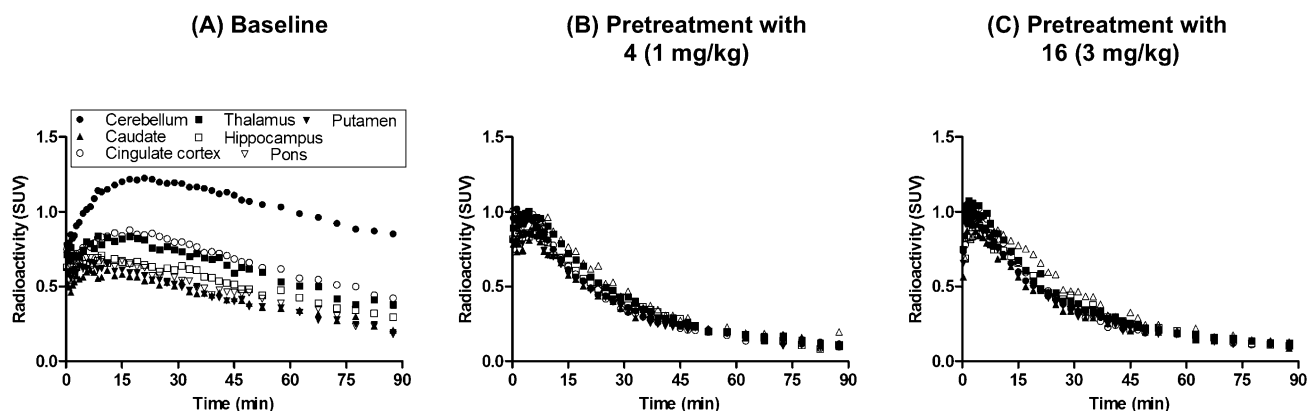
(A) Baseline | **(B) Pretreatment with 4 (1 mg/kg)** | **(C) Pretreatment with 16 (3 mg/kg)**

Figure 5. Time−activity curves of PET with $[^{11}C]4$ in the cerebellum (filled circles), thalamus (filled squares), hippocampus (blank squares), putamen (filled down-triangles), caudate (filled up-triangles), cingulate cortex (blank circles), and pons (blank down-triangles) of monkey brain: (A) $[^{11}C]4$ only; (B) $[^{11}C]4$ after treatment with 4 (1 mg/kg); (C) $[^{11}C]4$ after treatment with 16 (3 mg/kg).

Table 3. Area under the Curve (AUC, SUV × min) Values of $[^{11}C]4$ with Vehicle (C_T) or Unlabeled 4 (C_{ND}) in Monkey Brain

region	$\int C_T$	$\int C_{ND}$	DVR
cerebellum	91.9	31.5	4.3
thalamus	54.3	33.9	2.0
hippocampus	44.7	31.1	1.8
caudate	36.8	29.2	1.5
putamen	37.2	28.8	1.5
cingulate cortex	58.8	30.3	2.6
pons	40.0	35.6	1.0

state using the noninvasive Logan reference method (Logan Ref)[33] from the AUC in the blocking experiment ($\int C_{ND}$) as a reference, because this AUC indicated the nondisplaceable volume only. The results of liner regression with Logan Ref are shown in Supporting Information Figure 3.

As shown in Table 3, the DVR in the cerebellum was found to be 4.3 while the values in the other regions were in the range 1.0−2.6. The DVR in the pons was 1.0, indicating that the distribution volume (V_T) of the pons was equal to that of the reference (V_{ND}). This result suggested that the pons could be used as a reference tissue for performing quantitative PET analysis. In further PET experiments with $[^{11}C]4$, the validation study will be performed to assess the usefulness of the reference tissue methods for quantitative analysis by comparing with the invasive method using arterial blood sampling.

Metabolite Analysis. Table 4 shows the percentages of unchanged $[^{11}C]4$ measured by radio-HPLC in the plasma and brain homogenate of rat and the plasma of monkey. After the injection of $[^{11}C]4$ into rats, the fraction in the plasma corresponding to $[^{11}C]4$ decreased throughout the experiment,

Table 4. Percentages of Fraction of Unchanged $[^{11}C]4$ in Rat Plasma and Brain and Monkey Plasma

time after injection (min)	rat ($n = 3$)		monkey plasma
	brain	plasma	
5	94.0 ± 1.8	67.9 ± 5.8	70.2
15	95.2 ± 1.4	47.6 ± 4.4	43.1
30	97.0 ± 0.9	39.0 ± 3.8	35.8
60	98.2 ± 0.6	33.9 ± 3.2	28.4

with only 34% of the total radioactivity at 60 min. Two radiolabeled metabolites were observed in the HPLC chromatograms of the plasma samples. As indicated by their retention times (t_R) of 3.4 and 4.6 min, both metabolites were more polar than $[^{11}C]4$ ($t_R = 7.1$ min). On the other hand, the radioactivity in the brain homogenate was found to represent unchanged $[^{11}C]4$ with minor radiolabeled metabolites (<5%) at 60 min. Because the treated brain homogenate might be slightly contaminated with the blood of brain capillaries, percentages of the radiolabeled metabolites in the brain tissue would be smaller than the experimentally found values.

Metabolite analysis was also performed in monkey plasma. The fraction of unchanged $[^{11}C]4$ in the plasma at 5 and 60 min after the injection decreased to 70% and 28%, respectively. The two radiolabeled metabolites previously found in the rat plasma were also found in the monkey plasma. Because of very low levels of these radiolabeled metabolites in the rat brain homogenate, it could be assumed that these metabolites were hardly included in the monkey brain, suggesting that the specific binding for mGlu1 visualized in the brain was due to $[^{11}C]4$ and was not reflective of any radiolabeled metabolites.

The current results indicate that $[^{11}C]4$ is a useful PET ligand for the imaging and quantitative analysis of brain mGlu1 receptor. In PET studies for the same monkey, $[^{11}C]4$ showed improved kinetics in brain over $[^{18}F]1$. Although $[^{18}F]1$ showed higher brain uptake than $[^{11}C]4$, decreasing rates of radioactivity for $[^{18}F]1$ were much slower than those for $[^{11}C]4$ across the brain regions studied.[19] The DVR value for $[^{18}F]1$ in the pons, a negligible region for mGlu1, of monkey brain was 1.4, whereas the value for $[^{11}C]4$ in the same region was 1.0. Improvement in the brain kinetics may be related to moderate lipophilicity (cLogD = 2.67) and decreased binding affinity for mGlu1 (K_i = 13.6 nM) of $[^{11}C]4$ compared to that of $[^{18}F]1$ (K_i = 5.4 nM),[18] which could contribute to clearance of $[^{11}C]4$ from brain tissue following release from the mGlu1-binding sites.

A comparison of the results from the metabolite analyses revealed the superiority of $[^{11}C]4$ over $[^{11}C]2$. Less than 5% of total radioactivity in the rat brain represented the radiolabeled metabolites of $[^{11}C]4$ at 60 min after the injection, suggesting that radioactive signals in the brain almost contribute to $[^{11}C]4$ itself. On the other hand, around 20% of the total radioactivity in the rat brain represented the metabolite of $[^{11}C]2$ at 60 min.[18] These findings indicated that the replacement of the O-$[^{11}C]$methyl group in $[^{11}C]2$ with the C-$[^{11}C]$methyl group in $[^{11}C]4$ limited the entry of the resulting radiolabeled metabolites

to brain. The results supported PET with [^{11}C]**4** as being a feasible tool for the quantitative measurement of mGlu1 in the brains.

■ SUMMARY

In the current study, we have synthesized three novel mGlu1 ligands **3**–**5**. Of these ligands, compound **4** showed high in vitro binding affinity for mGlu1 together with a suitable lipophilicity. [^{11}C]**4** was synthesized via the *C*-[^{11}C]methylation of the arylstannane precursor **11** with [^{11}C]MeI in a short synthesis time and reliable radiochemical yield. PET study of monkey brain with [^{11}C]**4** showed a relatively high uptake and indicated that the radiolabeled metabolites in the plasma were hardly included in the brain. This study has succeeded in discovering a useful PET ligand [^{11}C]**4** ([^{11}C]ITDM) which represents a promising tool for the quantitative analysis of mGlu1 and merits further evaluation in human subjects.

■ EXPERIMENTAL SECTION

Materials and Methods. Melting points were measured using a micromelting point apparatus (MP-500P, Yanaco, Tokyo, Japan) and are uncorrected. ^{1}H NMR (300 MHz) spectra were recorded on a JEOL-AL-300 spectrometer (JEOL, Tokyo) using tetramethylsilane (TMS) as an internal standard. All chemical shifts (δ) have been reported in parts per million (ppm) downfield relative to the TMS signal. Signals are quoted as s (singlet), d (doublet), t (triplet), br (broad), or m (multiplet). Fast atom bombardment mass spectra and high-resolution mass spectra were obtained and recorded on a JEOL-AL-300 spectrometer (JEOL). Silica gel column chromatography was performed using Wako gel C-200 (70−230 mesh, Wako Pure Chemical Industries, Osaka, Japan). HPLC analysis was performed using the JASCO HPLC system (JASCO, Tokyo) and Capcell Pack C$_{18}$ column (4.6 mm i.d. × 250 mm, Shiseido, Tokyo). The chemical purities (≥95%) of compounds **3**−**5** and **11** were determined using analytical HPLC under the following conditions and were found to be more than 95%: 1.0 mL/min, acetonitrile (MeCN)/H$_2$O/triethylamine (Et$_3$N), 6/4/0.01 (v/v/v), for **3**−**5**; 2.0 mL/min, MeCN only for **11**. The radiochemical purity of [^{11}C]**4** was analyzed using HPLC with a detector for monitoring radioactivity under the following conditions: 1.0 mL/min, MeCN/H$_2$O/Et$_3$N (6/4/0.01, v/v/v). Under HPLC separation and analysis, effluent radioactivity was monitored using a NaI (Tl) scintillation detector system. All chemical reagents and solvents were purchased from commercial sources (Sigma-Aldrich, St. Louis, MO; Wako Pure Chemical Industries and Tokyo Chemical Industries, Tokyo) and used as supplied. Compound **16** was purchased from Alexis Biochemicals (San Diego, CA).

Carbon-11 (^{11}C) was produced by a ^{14}N (p, α) ^{11}C nuclear reaction using a CYPRIS HM-18 cyclotron (Sumitomo Heavy Industry, Tokyo). If not otherwise stated, radioactivity was measured with an IGC-3R curiemeter (Aloka, Tokyo). For the in vitro binding assay, [^{18}F]**1** and [^{11}C]**10** were prepared according to the procedures described previously.[20,22]

Chemical Synthesis. 4-Chloro-*N*-[4-[6-(isopropylamino)-pyrimidin-4-yl]-1,3-thiazol-2-yl]-*N*-methylbenzamide (3). To a solution of **7** (200 mg, 0.55 mmol) and K$_2$CO$_3$ (115 mg, 0.83 mmol) in 1,4-dioxane (12 mL) was added isopropylamine (1 mL, 11.7 mmol) at room temperature, and the resulting reaction mixture was heated at 80 °C for 7 h. The mixture was quenched with water and extracted with CH$_2$Cl$_2$. The organic layer was washed with brine, dried over Na$_2$SO$_4$, and evaporated under reduced pressure. The residue was purified by column chromatography using *n*-hexane/ethyl acetate/Et$_3$N (1/1/0.002, v/v/v) to give **3** (125 mg, 58.6%) as a colorless solid, mp 192−193 °C. ^{1}H NMR (CDCl$_3$): δ 1.29 (6H, d, *J* = 6.2 Hz), 3.74 (3H, s), 4.12 (1H, br), 4.87 (1H, br), 7.05 (1H, s), 7.52 (4H, m), 7.93 (1H, s), 8.57 (1H, s). HRMS *m/z* 388.0980 (calcd for C$_{18}$H$_{19}$ON$_5$ClS: 388.0999).

***N*-[4-[6-(Isopropylamino)pyrimidin-4-yl]-1,3-thiazol-2-yl]-*N*,4-dimethylbenzamide (4).** To a solution of **8** (400 mg, 1.16 mmol) and K$_2$CO$_3$ (332 mg, 2.40 mmol) in 1,4-dioxane (15 mL) was added

isopropylamine (1 mL, 11.7 mmol) at room temperature, and the resulting mixture was heated at 80 °C for 8 h. The mixture was treated as described for the synthesis of **3**. Purification by column chromatography using *n*-hexane/ethyl acetate/Et$_3$N (1/1/0.002, v/v/v) gave **4** (294 mg, 66.7%) as a colorless powder, mp 199−201 °C. ^{1}H NMR (CDCl$_3$): δ 1.29 (6H, d, *J* = 6.6 Hz), 2.44 (3H, s), 3.75 (3H, s), 4.11 (1H, br), 4.88 (1H, br), 7.06 (1H, s), 7.30 (2H, d, *J* = 7.7 Hz), 7.49 (2H, d, *J* = 8.1 Hz), 7.91 (1H, s), 8.57 (1H, s). HRMS *m/z* 368.1516 (calcd for C$_{19}$H$_{22}$ON$_5$S: 368.1545).

4-Cyano-*N*-[4-[6-(isopropylamino)pyrimidin-4-yl]-1,3-thia-zol-2-yl]-*N*-methylbenzamide (5). To a solution of **9** (356 mg, 1.00 mmol) and K$_2$CO$_3$ (207 mg, 1.50 mmol) in 1,4-dioxane (15 mL) was added isopropylamine (1 mL, 11.7 mmol) at room temperature, and the resulting mixture was heated at 80 °C for 7 h. The mixture was treated as described for the synthesis of **3**. Purification by column chromatography using *n*-hexane/ethyl acetate/Et$_3$N (1/2/0.003, v/v/v) gave **5** (232 mg, 61.3%) as a colorless powder, mp 214−215 °C. ^{1}H NMR (CDCl$_3$): δ 1.29 (6H, d, *J* = 6.6 Hz), 3.71 (3H, s), 4.11 (1H, br), 4.89 (1H, br), 7.03 (1H, s), 7.69 (2H, d, *J* = 8.1 Hz), 7.83 (2H, d, *J* = 8.1 Hz), 7.96 (1H, s), 8.57 (1H, s). HRMS *m/z* 379.1318 (calcd for C$_{19}$H$_{19}$ON$_6$S: 379.1341).

4-Chloro-*N*-[4-(6-chloropyrimidin-4-yl)-1,3-thiazol-2-yl]-*N*-methylbenzamide (7). A mixture of **6** (150 mg, 0.66 mmol), Et$_3$N (202 mg, 2.00 mmol), and 4-chlorobenzoyl chloride (173 mg, 0.99 mmol) in toluene (5 mL) was heated at 100 °C for 7 h under a N$_2$ atmosphere. This mixture was quenched with water and extracted with CH$_2$Cl$_2$. The organic layer was dried over Na$_2$SO$_4$ and evaporated under reduced pressure. The residue was purified by column chromatography using CH$_2$Cl$_2$/Et$_3$N (1/0.001, v/v) and then CH$_2$Cl$_2$/ethyl acetate/Et$_3$N (4/1/0.005, v/v/v) to give **7** (216 mg, 89.6%) as a colorless powder, mp 198−200 °C. ^{1}H NMR (CDCl$_3$): δ 3.76 (3H, s), 7.53 (4H, m), 8.06 (1H, s), 8.13 (1H, s), 8.95 (1H, s). FAB−MS: *m/z* 365 [M + H]$^+$.

***N*-[4-(6-Chloropyrimidin-4-yl)-1,3-thiazol-2-yl]-*N*,4-dimethyl-benzamide (8).** A mixture of **6** (227 mg, 1.00 mmol), Et$_3$N (304 mg, 3.00 mmol), and 4-methylbenzoyl chloride (232 mg, 1.50 mmol) in toluene (6 mL) was heated at 100 °C for 3 h under a N$_2$ atmosphere. This mixture was treated as described for **7**. Purification by column chromatography using CH$_2$Cl$_2$/Et$_3$N (1/0.001, v/v) and then CH$_2$Cl$_2$/ethyl acetate/Et$_3$N (4/1/0.005, v/v/v) gave **8** (242 mg, 70.2%) as a colorless powder, mp 183−184 °C. ^{1}H NMR (CDCl$_3$): δ 2.45 (3H, s), 3.77 (3H, s), 7.32 (2H, d, *J* = 8.1 Hz), 7.51 (2H, d, *J* = 8.1 Hz), 8.06 (1H, s), 8.11 (1H, s), 8.95 (1H, s). FAB−MS: *m/z* 345 [M + H]$^+$.

4-Cyano-*N*-[4-(6-chloropyrimidin-4-yl)-1,3-thiazol-2-yl]-*N*-methylbenzamide (9). A mixture of **6** (113 mg, 0.50 mmol), Et$_3$N (152 mg, 1.50 mmol), and 4-cyanobenzoyl chloride (124 mg, 0.75 mmol) in toluene (5 mL) was heated at 100 °C for 8 h under a N$_2$ atmosphere. This mixture was treated as described for **7**. Purification by column chromatography using CH$_2$Cl$_2$/Et$_3$N (1/0.001, v/v) and then CH$_2$Cl$_2$/ethyl acetate/Et$_3$N (9/1/0.01, v/v/v) gave **9** (120 mg, 67.5%) as a colorless powder, mp 212−214 °C. ^{1}H NMR (CDCl$_3$): δ 3.74 (3H, s), 7.71 (2H, d, *J* = 8.1 Hz), 7.84 (2H, d, *J* = 8.1 Hz), 8.04 (1H, s), 8.15 (1H, s), 8.96 (1H, s). FAB−MS: *m/z* 356 [M + H]$^+$.

***N*-[4-[6-(Isopropylamino)pyrimidin-4-yl]-1,3-thiazol-2-yl]-*N*-methyl-4-(tributylstannyl)benzamide (11).** To a solution of **13** (150 mg, 0.24 mmol) and K$_2$CO$_3$ (50 mg, 0.36 mmol) in 1,4-dioxane (8 mL) was added isopropylamine (1 mL, 11.7 mmol) at room temperature, and the resulting mixture was heated at 80 °C for 6 h. The mixture was treated as described for the synthesis of **3**. Purification by column chromatography using *n*-hexane/ethyl acetate/Et$_3$N (1/1/0.002, v/v/v) gave **11** (109 mg, 70.8%) as a colorless powder, mp 107−109 °C. ^{1}H NMR (CDCl$_3$): δ 0.90 (9H, t, *J* = 7.3 Hz), 1.10 (6H, t, *J* = 7.7 Hz), 1.29 (6H, d, *J* = 6.2 Hz), 1.29−1.41 (6H, m), 1.51−1.61 (6H, m), 3.76 (3H, s), 4.13 (1H, br), 4.92 (1H, br), 7.07 (1H, s), 7.51 (2H, d, *J* = 8.1 Hz), 7.60 (2H, d, *J* = 8.1 Hz), 7.93 (1H, s), 8.58 (1H, s). HRMS *m/z* 644.2417 (calcd for C$_{30}$H$_{46}$ON$_5$SSn: 644.2445).

4-Bromo-*N*-[4-(6-chloropyrimidin-4-yl)-1,3-thiazol-2-yl]-*N*-methylbenzamide (12). A mixture of **6** (1.14 g, 5.0 mmol), Et$_3$N (1.52 g, 15.0 mmol), and 4-bromobenzoyl chloride (1.65 g, 7.5 mmol) in toluene (30 mL) was heated at 100 °C for 6 h under a N$_2$ atmosphere. This mixture was treated as described for **7**. Purification by column

chromatography using CH_2Cl_2/Et_3N (1/0.001, v/v) and then $CH_2Cl_2/$ethyl acetate/Et_3N (4/1/0.005, v/v/v) gave **12** (1.1 g, 53.7%) as a colorless powder, mp 225−226 °C. ^{1}H NMR ($CDCl_3$): δ 3.76 (3H, s), 7.48 (2H, d, J = 8.4 Hz), 7.68 (2H, d, J = 8.4 Hz), 8.06 (1H, s), 8.13 (1H, s), 8.95 (1H, s). HRMS m/z 408.9545 (calcd for $C_{15}H_{11}ON_4ClBrS$: 408.9525).

N-[4-(6-Chloropyrimidin-4-yl)-1,3-thiazol-2-yl]-N-methyl-4-(tributylstannyl)benzamide (13). *From 12.* A mixture of **12** (860 mg, 2.11 mmol), bis(tributyltin) (1.45 g, 2.50 mmol), K_2CO_3 (346 mg, 2.50 mmol), and $Pd(PPh_3)_4$ (121 mg, 0.11 mmol) in toluene (15 mL) was heated at 100 °C for 24 h under a N_2 atmosphere. This mixture was quenched with water and extracted with CH_2Cl_2. The organic layer was dried over Na_2SO_4 and evaporated under reduced pressure. The residue was purified by column chromatography using CH_2Cl_2/Et_3N (1/0.001, v/v) and then CH_2Cl_2/ethyl acetate/Et_3N (4/1/0.005, v/v/v) to give **13** (50 mg, 3.8%) as a colorless powder, mp 136−139 °C. ^{1}H NMR ($CDCl_3$): δ 0.90 (9H, t, J = 7.3 Hz), 1.10 (6H, t, J = 7.7 Hz), 1.29−1.41 (6H, m), 1.51−1.61 (6H, m), 3.78 (3H, s), 7.45−7.63 (4H, m), 7.88 (1H, s), 8.12 (1H, s), 8.68 (1H, s). FAB−MS: m/z 620 [M + H]+.

From 14. A mixture of **14** (1.24 g, 5.00 mmol), LiCl (1.05 g, 25 mmol), $Pd(PPh_3)_4$ (289 mg, 0.25 mmol), bis(tributyltin) (5.0 mL, 10.00 mmol) in 1,4-dioxane (40 mL) was heated at reflux for 17 h under a N_2 atmosphere. The reaction mixture was quenched with CH_2Cl_2/H_2O (1/1, v/v), and the solution was filtered through Celite with CH_2Cl_2. The organic layer was washed with water, dried over Na_2SO_4, and evaporated under reduced pressure. The residue was purified by flash chromatography using n-hexane/ethyl acetate (9/1, v/v) to give crude **15** (1.44 g).[26,27]

A mixture of **15** (760 mg), Et_3N (562 mg, 5.55 mmol), BOP (774 mg, 1.75 mmol), and **6** (340 mg, 1.50 mmol) in 1,4-dioxane (10 mL) was heated at 50 °C for 20 h under a N_2 atmosphere. The reaction mixture was quenched with water and extracted with CH_2Cl_2. The organic layer was dried over Na_2SO_4 and evaporated under reduced pressure. Purification by column chromatography using CH_2Cl_2/Et_3N (1/0.001, v/v) and then CH_2Cl_2/ethyl acetate/Et_3N (4/1/0.005, v/v/v) gave **13** (190 mg, 20.4%) as a colorless powder.

Radiochemistry. N-[4-[6-(Isopropylamino)pyrimidin-4-yl]-1,3-thiazol-2-yl]-N-methyl-4-[^{11}C]methylbenzamide ([^{11}C]4). K_2CO_3 (2.1 mg, 15 μmol), copper(I) chloride (1.5 mg, 15 μmol), and $Pd_2(dba)_3$ (1.3 mg, 1.4 μmol) were added to a minivial (1 mL) equipped with a septum and stirring bar. The vial was purged with N_2, and a solution of $P(o-tol)_3$ (1.7 mg, 5.6 μmol) in DMF (0.2 mL) was added. The resulting mixture was stirred for 5 min at room temperature before a solution of **11** (1.9 mg, 3 μmol) in DMF (0.1 mL) was added. This mixture was purged with N_2 and stirred for 1 min. The prepared solution was transferred with a syringe into a reaction vial equipped with the automated synthetic unit.[28]

After irradiation, the cyclotron-produced [^{11}C]CO_2 was bubbled into 0.4 M $LiAlH_4$ in anhydrous tetrahydrofuran (THF, 0.3 mL). After evaporation of THF, the remaining complex was treated with 57% hydroiodic acid (0.3 mL) to give [^{11}C]MeI, which was distilled with heating and transferred under N_2 gas flow into the above solution containing **11** at −15 to −20 °C. When the radioactivity of [^{11}C]MeI reached a plateau, the reaction mixture was heated at 80 °C for 5 min. After 1.0 mL of the preparative HPLC mobile phase was added, the final mixture was filtered with a glass fiber prefilter (GF53, 30 mm; Agilent Technologies, Santa Clara, CA) and applied to the HPLC system. HPLC separation was completed on a Capcell Pack C_{18} column (10 mm i.d. × 250 mm; Shiseido) using $MeCN/H_2O/Et_3N$ (6/4/0.01, v/v/v) at 5.0 mL/min. The radioactive fraction corresponding to [^{11}C]**4** (t_R = 10.4 min) was collected in a sterile flask, evaporated to dryness in vacuo, redissolved in 3 mL of sterile normal saline, and passed through a 0.22 μm Millipore filter to give 1.6 GBq [^{11}C]**4**. The identity of [^{11}C]**4** (t_R = 9.4 min) was confirmed by analytical HPLC with **4**. The specific activity was calculated by comparing the assayed radioactivity to the mass measured at UV 254 nm. The synthesis time was 31 min from EOB: radiochemical yield (decay-corrected), 28% based on [^{11}C]CO_2; radiochemical purity, >99%; specific activity at EOS, 170 GBq/μmol.

Computation and Measurement of Lipophilicity. The cLogD values of **3−5** were determined computationally using Pallas 3.4

software (CompuDrug, Sedona, AZ). The log D value was measured by mixing [^{11}C]**4** (radiochemical purity, 100%; about 200000 cpm) with n-octanol (3.0 g) and phosphate buffered saline (PBS; 3.0 g, 0.1 M, pH 7.4) in a test tube. The mixture was vortexed for 3 min at room temperature, followed by centrifugation at 2330g for 5 min. An aliquot of 1 mL of PBS and 1 mL of n-octanol was removed and weighed, and its radioactivity was counted with a 1480 Wizard automatic γ counter (Perkin-Elmer, Waltham, MA), respectively. Each sample from the remaining organic layer was removed and repartitioned until a consistent log D was obtained. The log D value was calculated by comparing the ratio of cpm/g n-octanol to that of PBS and expressed as log D = log[(cpm/g (n-octanol))/(cpm/g (PBS))]. All measurements were performed in triplicate.

Animal. DdY mice (male, 8 weeks old, 34−36 g) and Sprague−Dawley rats (male, 7−8 weeks old, 210−280 g) were purchased from Japan SLC (Shizuoka, Japan). These animals were housed under a 12 h dark−light cycle and were allowed free access to food pellets and water. The animal experiments were approved by the Animal Ethics Committee of the National Institute of Radiological Sciences.

In Vitro Binding Assays. Rats (n = 5) were sacrificed by decapitation under ether anesthesia. The whole brains were rapidly removed and homogenized in 10 volumes of 50 mM Tris-HCl (pH 7.4) containing 120 mM NaCl with a Silent Crusher S homogenizer (Heidolph Instruments, Schwabach, Germany). The homogenate was centrifuged in a polypropylene tube at 40000g for 15 min at 4 °C using an Optima-TLX (Beckman Coulter, Brea, CA). After the supernatant was discarded, the pellet was resuspended, homogenized, and centrifuged in the same buffer. This procedure was repeated twice to obtain the final pellet of brain homogenate, which was stored at −80 °C until experimental use.

The brain homogenate was diluted to 100 mg/mL in 50 mM Tris-HCl buffer containing 120 mM NaCl, 2 mM KCl, 1 mM $MgCl_2$, and 1 mM $CaCl_2$. Each preparation of 0.1 mL of homogenate was incubated with [^{18}F]**1** (3 nM in PBS) and 0.1 mL of the test compounds **3−5** (10^{-6} to 10^{-10} M in 0.1% dimethylsulfoxide) in a final volume of 1.0 mL of buffer. These mixtures were incubated for 1 h at room temperature. The bound and free radioligands were separated by vacuum filtration through 0.3% polyethylenimine-pretreated Whatman GF/C glass fiber filters using a cell harvester (M-24, Brandel, Gaithersburg, MD), followed by washing with prechilled buffer three times. The filters containing the bound [^{18}F]**1** were assayed for radioactivity in the automatic γ counter. Subsequently, we performed the same assay with [^{11}C]**10**, an antagonistic radioligand for mGlu5, as described above. The results of inhibitory experiments were subjected to nonlinear regression analysis using Prism 5 (GraphPad Software, La Jolla, CA) through which IC_{50} and the inhibition constant (K_i) values were calculated.

In Vitro Autoradiography. Rat brain sections (10 μm) were preincubated for 20 min in 50 mM Tris-HCl buffer (pH 7.4) containing 1.2 mM $MgCl_2$ and 2 mM $CaCl_2$ at room temperature. Following a period of preincubation, these sections were incubated for 60 min at room temperature in fresh buffer containing [^{11}C]**4** (9.2 MBq, 0.5 nM). Compound **16** (1 μM) was used to determine the specific binding of [^{11}C]**4** for mGlu1. After incubation, these brain sections were washed (3 × 2 min) with cold buffer, dipped in cold distilled water, and dried with cold air. These sections were placed in contact with imaging plates (BAS-MS2025, Fujifilm, Tokyo), and autoradiograms were obtained using a Bio-Imaging analyzer system (BAS5000, Fujifilm).

Biodistribution Study in Mice. A saline solution of [^{11}C]**4** (4.8 MBq/0.1 mL, 40 pmol) was injected into mice through the tail vein. Four mice were sacrificed per time point at 1, 5, 15, 30, 60, and 90 min after the injection by cervical dislocation. The whole brain, heart, liver, lung, spleen, pancreas, testis, kidney, small intestine (including contents), large intestine (including contents) muscle, and blood samples were quickly removed. Radioactivity present in these tissues was measured with the automatic γ counter and expressed as the percentage of injected dose per gram of wet tissue (%ID/g). All radioactivity measurements were decay-corrected.

PET Study in Monkey. Prior to the PET assessments, MRI was performed on a monkey brain with a Signa EXCITE HD at 3.0 T (GE Medical Systems, Milwaukee, WI) and a short time inversion recovery

sequence (repetition time = 5000 ms, echo time = 80 ms, inversion time = 110 ms, FOV = 100 mm, number of slices = 52, slice thickness = 1 mm without slice gap, 512 × 384 acquisition matrix, which after reconstruction was reformatted to a 512 × 512 image matrix, number of excitations = 6, total acquisition time = 72 min).[34]

PET scans were performed using a high resolution SHR-7700 PET camera (Hamamatsu Photonics, Hamamatsu, Japan) designed for laboratory animals. This camera could provide 31 horizontal slices that were 3.6 mm (center-to-center) apart with a 33.1 cm FOV. A male rhesus monkey was anesthetized with ketamine. Transmission scans for attenuation correction were subsequently performed using a 74 MBq $^{68}Ge^{68}Ga$ source. Emission scan images were reconstructed with a 4.0 mm Colsher filter, and circular volumes of interest (VOIs) with a 5 mm diameter were placed over the frontal cortex, cingulate cortex, caudate, putamen, hippocampus, thalamus, cerebellum, and pons using PMOD, version 3.2 (PMOD Technologies, Zurich, Switzerland).

A solution of $[^{11}C]\mathbf{4}$ (185−220 MBq, 5−6 nmol, 0.5−1 mL) was injected intravenously into the monkey, and time-sequential tomographic scanning was performed for 90 min on a horizontal section of the brain. For the inhibitory study, the same monkey was injected with unlabeled **4** (1 mg/kg) or **16** (3 mg/kg) 30 s prior to the injection of $[^{11}C]\mathbf{4}$ and 2 weeks after the baseline study. PET images were obtained by summing the uptakes between 10 and 90 min. VOIs were placed on each brain region using image analysis software PMOD (PMOD Technologies) with reference to the MRI template. Each PET image was overlaid on the MRI template, and the TAC for each region was characterized. Brain uptake was decay-corrected to the injection time and expressed as SUV, which was normalized to the injected radioactivity and body weight. SUV = (radioactivity per milliliter tissue/injected radioactivity) × gram body weight.

Noninvasive graph analyses using Logan Ref were performed in each region by PMOD (PMOD Technologies) using the TAC from both the baseline and blocking experiment with unlabeled **4**. The DVRs were directly calculated from the graphical method using AUC ($\int C_{ND}$) of the blocking as a reference with an average tissue-to-plasma clearance k_2'. The average k_2' in each region was estimated from simplified reference tissue model[35] analysis using the TAC in the blocking instead of the reference tissue.

This treatment resulted in the following linear regression equation:

$$\frac{\int C_T \, dt}{C} = DVR \left[\frac{\int C_{ND} \, dt + C'/k_2'}{C} \right] + int'$$

which contains DVR as the regression slope and an intercept int' that becomes constant following an equilibration time t^*.

Metabolite Assay for Rat and Monkey Plasma and Rat Brain. After the intravenous injection of $[^{11}C]\mathbf{4}$ (37 MBq/0.1 mL), the rats (n = 3) were sacrificed by cervical dislocation at 5, 15, 30, or 60 min. Blood (0.7−1.0 mL) and whole brain samples were quickly removed, and the blood samples were centrifuged at 15000 rpm for 1 min at 4 °C to separate the plasma. The supernatant (0.5 mL) was then collected in a test tube containing MeCN (0.5 mL), and the resulting mixture was vortexed for 15 s and centrifuged at 15000 rpm for 2 min for deproteinization. The resulting supernatant was collected. Subsequently, the rat brain was homogenized with a Silent Crusher S homogenizer in an ice-cooled MeCN/H$_2$O (1/1, 2.0 mL) solution. The resulting homogenate was then centrifuged at 15000 rpm for 2 min at 4 °C. The supernatant (0.5 mL) was collected and resuspended with MeCN (0.5 mL) and then centrifuged at 15000 rpm for 2 min at 4 °C for deproteinization.

Following the injection of $[^{11}C]\mathbf{4}$ (185 MBq/mL) into the monkey, arterial blood samples (1 mL) were collected at 5, 15, 30, and 60 min. The treated versions of these samples were acquired according to the same procedure described above.

An aliquot of the supernatant (0.3−0.8 mL) obtained from the plasma or brain homogenate was injected into the HPLC system with a radioactivity detector[36] and analyzed using a Capcell Pack C$_{18}$ column (4.6 mm i.d. × 250 mm) with MeCN/H$_2$O/Et$_3$N (7/3/0.01, v/v/v) at 1.0 mL/min. The percentage of $[^{11}C]\mathbf{4}$ (t_R = 7.1 min) to total radioactivity (corrected for decay) on the HPLC chromatogram was calculated as % = (peak area for $[^{11}C]\mathbf{4}$/total peak area) × 100.

■ ASSOCIATED CONTENT

⑤ Supporting Information

Purities of **3−5** and **11** determined by HPLC; HPLC analytic charts for **3−5** and **11**; noninvasive Logan graphical analyses; chemical structures of $[^{11}C]\mathbf{10}$ and **16**. This material is available free of charge via the Internet at http://pubs.acs.org.

■ AUTHOR INFORMATION

Corresponding Author

*Address: Department of Molecular Probes, Molecular Imaging Center, National Institute of Radiological Sciences, 4-9-1 Anagawa, Inage-ku, Chiba 263-8555, Japan. Phone: +81-43-382-3707. Fax: +81-43-206-3261. E-mail: zhang@nirs.go.jp.

Notes

The authors declare no competing financial interest.

■ ACKNOWLEDGMENTS

■ ABBREVIATIONS USED

AUC, area under the curve; BBB, blood−brain barrier; BOP, (benzotriazol-1-yloxy)tris(dimethylamino)phosphonium hexafluorophosphate; CNS, central nervous system; $[^{11}C]CO_2$, $[^{11}C]$carbon dioxide; DMF, N,N-dimethylformamide; DVR, distribution volume ratio; EOB, end of bombardment; EOS, end of synthesis; Et$_3$N, triethylamine; FAB-MS, fast atom bombardment mass spectrometry; HPLC, high performance liquid chromatography; HRMS, high resolution mass spectrometry; %ID/g, percentage of the injected dose per gram of wet tissue; K_i, inhibition constant; LiAlH$_4$, lithium aluminum hydride; Logan Ref, Logan reference method; MeCN, acetonitrile; $[^{11}C]$MeI, $[^{11}C]$methyl iodide; mGlu1, metabotropic glutamate receptor type 1; mGlu5, metabotropic glutamate receptor type 5; PBS, phosphate buffered saline; Pd$_2$(dba)$_3$, tris-(dibenzylideneacetone)dipalladium(0); Pd(PPh$_3$)$_4$, tetrakis-(triphenylphosphine)palladium(0); PET, positron emission tomography; SUV, standardized uptake value; TAC, time−activity curve; t_R, retention time; V_{ND}, distribution volume of reference; V_T, distribution volume of tissue

■ REFERENCES

(1) Conn, P. J.; Pin, J. P. Pharmacology and functions of metabotropic glutamate receptors. *Annu. Rev. Pharmacol. Toxicol.* **1997**, *37*, 205−237.

(2) Nakanishi, S. Metabotropic glutamate receptors: synaptic transmission, modulation, and plasticity. *Neuron* **1994**, *13*, 1031−1037.

(3) Bordi, F.; Ugolini, A. Group I metabotropic glutamate receptors: implications for brain diseases. *Prog. Neurobiol.* **1999**, *59*, 55−79.

(4) Ferraguti, F.; Crepaldi, L.; Nicoletti, F. Metabotropic glutamate 1 receptor: current concepts and perspectives. *Pharmacol. Rev.* **2008**, *60*, 536−581.

(5) Kew, J. N.; Kemp, J. A. Ionotropic and metabotropic glutamate receptor structure and pharmacology. *Psychopharmacology* **2005**, *179*, 4−29.

(6) Swanson, C. J.; Bures, M.; Johnson, M. P.; Linden, A. M.; Monn, J. A.; Schoepp, D. D. Metabotropic glutamate receptors as novel targets for anxiety and stress disorders. *Nat. Rev. Drug Discovery* **2005**, *4*, 131−144.

(7) Kaneda, K.; Imanishi, M.; Nambu, A.; Shigemoto, R.; Takada, M. Differential expression patterns of mGlu1 alpha in monkey nigral dopamine neurons. *NeuroReport* **2003**, *14*, 947−950.

(8) Kaneda, K.; Tachibana, Y.; Imanishi, M.; Kita, H.; Shigemoto, R.; Nambu, A.; Takada, M. Down-regulation of metabotropic glutamate receptor 1alpha in globus pallidus and substantia nigra of parkinsonian monkeys. *Eur. J. Neurosci.* **2005**, *22*, 3241−3254.

(9) Ribeiro, F. M.; Paquet, M.; Ferreira, L. T.; Cregan, T.; Swan, P.; Cregan, S. P.; Ferguson, S. S. Metabotropic glutamate receptor-mediated cell signaling pathways are altered in a mouse model of Huntington's disease. *J. Neurosci.* **2010**, *30*, 316−324.

(10) Werner, C. G.; Scartabelli, T.; Pancani, T.; Landucci, E.; Moroni, F.; Pellegrini-Giampietro, D. E. Differential role of mGlu1 and mGlu5 receptors in rat hippocampal slice models of ischemic tolerance. *Eur. J. Neurosci.* **2007**, *25*, 3597−3604.

(11) Zhou, M.; Xu, W.; Liao, G.; Bi, X.; Baudry, M. Neuroprotection against neonatal hypoxia/ischemia-induced cerebral cell death by prevention of calpain-mediated mGlu1alpha truncation. *Exp. Neurol.* **2009**, *218*, 75−82.

(12) Wang, J.; Maurer, L. Positron emission tomography: applications in drug discovery and drug development. *Curr. Top. Med. Chem.* **2005**, *5*, 1053−1075.

(13) Fujinaga, M.; Maeda, J.; Yui, J.; Hatori, A.; Yamasaki, T.; Kawamura, K.; Kumata, K.; Yoshida, Y.; Nagai, Y.; Higuchi, M.; Suhara, T.; Fukumura, T.; Zhang, M.-R. Characterization of 1-(2-[^{18}F]fluoro-3-pyridyl)-4-(2-isopropyl-1-oxo-isoindoline-5-yl)-5-methyl-1*H*-1,2,3-triazole, a PET ligand for imaging the metabotropic glutamate receptor type 1 in rat and monkey brains. *J. Neurochem.* **2012**, *121*, 115−124.

(14) Fujinaga, M.; Yamasaki, T.; Kawamura, K.; Kumata, K.; Hatori, A.; Yui, J.; Yanamoto, K.; Yoshida, Y.; Ogawa, M.; Nengaki, N.; Maeda, J.; Fukumura, T.; Zhang, M.-R. Synthesis and evaluation of 6-[1-(2-[^{18}F]fluoro-3-pyridyl)-5-methyl-1*H*-1,2,3-triazol-4-yl]quinoline for positron emission tomography imaging of the metabotropic glutamate receptor type 1 in brain. *Bioorg. Med. Chem.* **2011**, *19*, 102−110.

(15) Hostetler, E. D.; Eng, W.; Joshi, A. D.; Sanabria-Bohorquez, S.; Kawamoto, H.; Ito, S.; O'Malley, S.; Krause, S.; Ryan, C.; Patel, S.; Williams, M.; Riffel, K.; Suzuki, G.; Ozaki, S.; Ohta, H.; Cook, J.; Burns, H. D.; Hargreaves, R. Synthesis, characterization, and monkey PET studies of [^{18}F]MK-1312, a PET tracer for quantification of mGluR1 receptor occupancy by MK-5435. *Synapse* **2011**, *65*, 125−135.

(16) Prabhakaran, J.; Majo, V. J.; Milak, M. S.; Kassir, S. A.; Palner, M.; Savenkova, L.; Mali, P.; Arango, V.; Mann, J. J.; Parsey, R. V.; Kumar, J. S. Synthesis, in vitro and in vivo evaluation of [^{11}C]MMTP: a potential PET ligand for mGlu1 receptors. *Bioorg. Med. Chem. Lett.* **2011**, *20*, 3499−3501.

(17) Yanamoto, K.; Konno, F.; Odawara, C.; Yamasaki, T.; Kawamura, K.; Hatori, A.; Yui, J.; Wakizaka, H.; Nengaki, N.; Takei, M.; Zhang, M.-R. Radiosynthesis and evaluation of [^{11}C]YM-202074 as a PET ligand for imaging the metabotropic glutamate receptor type 1. *Nucl. Med. Biol.* **2010**, *37*, 615−624.

(18) Fujinaga, M.; Yamasaki, T.; Yui, J.; Hatori, A.; Xie, L.; Kawamura, K.; Asagawa, C.; Kumata, K.; Yoshida, Y.; Ogawa, M.; Nengaki, N.; Fukumura, T.; Zhang, M.-R. Synthesis and evaluation of novel radioligands for positron emission tomography imaging of metabotropic glutamate receptor subtype 1 (mGluR1) in rodent brain. *J. Med. Chem.* **2012**, *55*, 2342−2352.

(19) Yamasaki, T.; Fujinaga, M.; Maeda, J.; Kawamura, K.; Yui, J.; Hatori, A.; Yoshida, Y.; Nagai, Y.; Tokunaga, M.; Higuchi, M.; Suhara, T.; Fukumura, T.; Zhang, M.-R. Imaging for metabotropic glutamate receptor subtype 1 in rat and monkey brains using PET with [^{18}F]FITM. *Eur. J. Nucl. Med. Mol. Imaging* **2011**, *39*, 632−641.

(20) Yamasaki, T.; Fujinaga, M.; Yoshida, Y.; Kumata, K.; Yui, J.; Kawamura, K.; Hatori, A.; Fukumura, T.; Zhang, M.-R. Radiosynthesis and preliminary evaluation of 4-[^{18}F]fluoro-*N*-[4-[6-(isopropylamino)-pyrimidin-4-yl]-1,3-thiazol-2-yl]-*N*-methylbenzamide as a new positron emission tomography ligand for metabotropic glutamate receptor subtype 1. *Bioorg. Med. Chem. Lett.* **2011**, *21*, 2998−3001.

(21) Yamasaki, T.; Fujinaga, M.; Kawamura, K.; Yui, J.; Hatori, A.; Ohya, T.; Xie, L.; Wakizaka, H.; Yoshida, Y.; Fukumura, T.; Zhang, M.-R. In vivo measurement of the affinity and density of metabotropic glutamate receptor subtype 1 (mGluR1) in rat brain using ^{18}F-FITM in small-animal PET. *J. Nucl. Med.* **2012**, *53*, 1601−1607.

(22) Ametamey, S. M.; Kessler, L. J.; Honer, M.; Wyss, M. T.; Buck, A.; Hintermann, S.; Auberson, Y. P.; Gasparini, F.; Schubiger, P. A. Radiosynthesis and preclinical evaluation of ^{11}C-ABP688 as a probe for imaging the metabotropic glutamate receptor subtype 5. *J. Nucl. Med.* **2006**, *47*, 698−705.

(23) Pike, V. W. PET radiotracers: crossing the blood−brain barrier and surviving metabolism. *Trends. Pharmacol. Sci.* **2009**, *30*, 431−440.

(24) Wilson, A. A.; Jin, L.; Garcia, A.; DaSilva, J. N.; Houle, S. An admonition when measuring the lipophilicity of radiotracers using counting techniques. *Appl. Radiat. Isot.* **2001**, *54*, 203−208.

(25) Suzuki, M.; Doi, H.; Bjorkman, M.; Andersson, Y.; Langstrom, B.; Watanabe, Y.; Noyori, R. Rapid coupling of methyl iodide with aryltributylstannanes mediated by palladium(0) complexes: a general protocol for the synthesis of ^{11}CH$_3$-labeled PET tracers. *Chem.—Eur. J.* **1997**, *3*, 2039−2042.

(26) Koziorowski, J.; Henssen, C.; Weinreich, R. A new convenient route to radioiodinated *N*-succinimidyl 3- and 4-iodobenzoate, two reagents for radioiodination of proteins. *Appl. Radiat. Isot.* **1998**, *49*, 955−959.

(27) Kaderavek, J.; Kozempel, J.; Sticha, M.; Petrasek, J.; Jirsa, M.; Taimr, P.; Leseticky, L. Vitamin a derivatives labelled with ^{131}I-potential agents for liver scintigraphy. *Czech. J. Phys.* **2006**, *56*, D711−D717.

(28) Suzuki, K.; Inoue, O.; Hashimoto, K.; Yamasaki, T.; Kuchiki, M.; Tamate, K. Computer-controlled large scale production of high specific activity [^{11}C]Ro 15-1788 for PET studies of benzodiazepine receptors. *Int. J. Appl. Radiat. Isot.* **1985**, *36*, 971−976.

(29) Lavreysen, H.; Wouters, R.; Bischoff, F.; Nobrega Pereira, S.; Langlois, X.; Blokland, S.; Somers, M.; Dillen, L.; Lesage, A. S. JNJ16259685, a highly potent, selective and systemically active mGlu1 receptor antagonist. *Neuropharmacology* **2004**, *47*, 961−972.

(30) Fotuhi, M.; Sharp, A. H.; Glatt, C. E.; Hwang, P. M.; von Krosigk, M.; Snyder, S. H.; Dawson, T. M. Differential localization of phosphoinositide-linked metabotropic glutamate receptor (mGluR1) and the inositol 1,4,5-trisphosphate receptor in rat brain. *J. Neurosci.* **1993**, *13*, 2001−2012.

(31) Lavreysen, H.; Pereira, S. N.; Leysen, J. E.; Langlois, X.; Lesage, A. S. Metabotropic glutamate 1 receptor distribution and occupancy in the rat brain: a quantitative autoradiographic study using [^{3}H]R214127. *Neuropharmacology* **2004**, *46*, 609−619.

(32) Innis, R. B.; Cunningham, V. J.; Delforge, J.; Fujita, M.; Gjedde, A.; Gunn, R. N.; Holden, J.; Houle, S.; Huang, S. C.; Ichise, M.; Iida, H.; Ito, H.; Kimura, Y.; Koeppe, R. A.; Knudsen, G. M.; Knuuti, J.; Lammertsma, A. A.; Laruelle, M.; Logan, J.; Maguire, R. P.; Mintun, M. A.; Morris, E. D.; Parsey, R.; Price, J. C.; Slifstein, M.; Sossi, V.; Suhara, T.; Votaw, J. R.; Wong, D. F.; Carson, R. E. Consensus nomenclature for in vivo imaging of reversibly binding radioligands. *J. Cereb. Blood Flow Metab.* **2007**, *27*, 1533−1539.

(33) Logan, J.; Fowler, J. S.; Volkow, N. D.; Wang, G. J.; Ding, Y. S.; Alexoff, D. L. Distribution volume ratios without blood sampling from graphical analysis of PET data. *J. Cereb. Blood Flow Metab.* **1996**, *16*, 834−840.

(34) Yui, J.; Maeda, J.; Kumata, K.; Kawamura, K.; Yanamoto, K.; Hatori, A.; Yamasaki, T.; Nengaki, N.; Higuchi, M.; Zhang, M.-R. ^{18}F-FEAC and ^{18}F-FEDAC: PET of the monkey brain and imaging of translocator protein (18 kDa) in the infarcted rat brain. *J. Nucl. Med.* **2010**, *51*, 1301−1309.

(35) Lammertsma, A. A.; Hume, S. P. Simplified reference tissue model for PET receptor studies. *NeuroImage* **1996**, *4*, 153−158.

(36) Takei, M.; Kida, T.; Suzuki, K. Sensitive measurement of positron emitters eluted from HPLC. *Appl. Radiat. Isot.* **2001**, *55*, 229−234.